*5834–5849* *Nucleic Acids Research, 2022, Vol. 50, No. 10* *Published online 17 May 2022*
*https://doi.org/10.1093/nar/gkac359*

# Lineage-specific insertions in T-box riboswitches modulate antibiotic binding and action

**Nikoleta Giarimoglou[1], Adamantia Kouvela[1], Ioanna Patsi[1], Jinwei Zhang[2], Vassiliki Stamatopoulou[1,*] and Constantinos Stathopoulos[1,*]**

[1]Department of Biochemistry, School of Medicine, University of Patras, 26504 Patras, Greece and [2]Laboratory of Molecular Biology, National Institute of Diabetes and Digestive and Kidney Diseases, NIH, Bethesda, MD 20892, USA

Received March 16, 2022; Revised April 21, 2022; Editorial Decision April 22, 2022; Accepted May 11, 2022

## ABSTRACT

**T-box riboswitches (T-boxes) are essential RNA regulatory elements with a remarkable structural diversity, especially among bacterial pathogens. In staphylococci, all *glyS* T-boxes synchronize glycine supply during synthesis of nascent polypeptides and cell wall formation and are characterized by a conserved and unique insertion in their antiterminator/terminator domain, termed stem Sa. Interestingly, in *Staphylococcus aureus* the stem Sa can accommodate binding of specific antibiotics, which in turn induce robust and diverse effects on T-box-mediated transcription. In the present study, domain swap mutagenesis and probing analysis were performed to decipher the role of stem Sa. Deletion of stem Sa significantly reduces both the *S. aureus glyS* T-box-mediated transcription readthrough levels and the ability to discriminate among $tRNA^{Gly}$ isoacceptors, both *in vitro* and *in vivo*. Moreover, the deletion inverted the previously reported stimulatory effects of specific antibiotics. Interestingly, stem Sa insertion in the terminator/antiterminator domain of *Geobacillus kaustophilus glyS* T-box, which lacks this domain, resulted in elevated transcription in the presence of tigecycline and facilitated discrimination among proteinogenic and nonproteinogenic $tRNA^{Gly}$ isoacceptors. Overall, stem Sa represents a lineage-specific structural feature required for efficient staphylococcal *glyS* T-box-mediated transcription and it could serve as a species-selective druggable target through its ability to modulate antibiotic binding.**

## INTRODUCTION

T-box riboswitches (T-boxes) represent a widespread class of *cis*-acting noncoding regulatory RNAs found predominantly in Gram-positive bacteria (1,2). They are transcribed as part of the 5′UTR of mRNAs that mainly code for aminoacyl-tRNA synthetases, amino acid transporters and enzymes that mediate amino acid metabolism (3,4). Their secondary structures are complex, exhibiting variability in length, stems and single-stranded regions (5). Most characterized T-boxes regulate transcription attenuation; however, T-boxes in Actinobacteria were recently found to conditionally sequester Shine–Dalgarno sequences to control translation initiation (6). A typical T-box consists of stem I, which includes the specifier loop that base pairs with the anticodon of the cognate tRNA ligand, an intervening linker of variable length that may also include stem II, a very important stem III that plays a role in the stabilization of the T-box:tRNA complex and the 3′ antiterminator/antisequestrator domain that includes the conserved T-box sequence that recognizes the universal 3′ CCA end of tRNAs (5,7–9). The antiterminator/antisequestrator domain, together with additional structural elements, is responsible for the structural shift between termination and antitermination of transcription or translation, which in turn relies on whether the bound tRNA is charged with its cognate amino acid or not. Both transcriptional and translational T-boxes can sense the aminoacylation status of tRNAs and therefore are considered key sensors of amino acid availability (10–13).

Since their discovery, progress toward better understanding the preconditions of the conformational switch of T-boxes was based on systematic and meticulous analysis of respective secondary structures using mainly chemical probing and enzymatic footprinting (14,15). As T-box-mediated regulation depends on the interaction of mRNA and tRNA, and resembles the same interaction on the ribosome, several questions have emerged regarding the evolution and conservation of T-boxes as RNA-mediated regulatory elements (16,17). Moreover, T-boxes are appealing molecular targets for the development of new antibacterials, especially considering that most clinically important human pathogens utilize T-boxes as regulators of their metabolism (18–20). Recent breakthrough studies on the *glyQ* T-box

*To whom correspondence should be addressed. Tel: +30 261 09 97 932; Email: cstath@med.upatras.gr
Correspondence may also be addressed to Vassiliki Stamatopoulou. Tel: +30 261 09 96 124; Email: v.stam@upatras.gr

from bacilli have shed light on the mechanism by which T-box-mediated transcription regulation is achieved (11). The tRNA ligand base pairs its anticodon with the codon-like triplet of the specifier loop and the apical loop of stem I can interact with the $tRNA^{Gly}$ 'elbow' (G19 of the D-loop and C56 of the T-loop) (8,17,21). Therefore, T-box acts as a molecular ruler to ensure a mutually induced fit mechanism, by which both RNAs change conformations to achieve shape complementarity (7,22). A third crucial interaction between the highly conserved sequence of the T-box bulge and the complementary 3′ CCA end of the tRNA is also important for the stabilization of the antiterminator conformation of the T-box favoring transcriptional 'readthrough' by the RNA polymerase (10,23–25). A comparison with the translational T-boxes, where stem I is short and does not interact with the tRNA's elbow, shows that stable binding of the tRNA is achieved by local, bridging contacts from the adjacent stem II S-turn (12,26). In both transcriptional and translational T-boxes, the non-aminoacylated 3′ end of the tRNA is enveloped inside a pocket created by the adjacent helices from the antiterminator/antisequestrator domain and stem III, which in combination with its adjoining purines stabilizes the discriminator to a more rigid structure. The 3′ end of an aminoacylated tRNA is hampered by a steric barrier created by the G167–U185 base pair, which prevents a critical stacking interaction between C186 and tA76 at the tRNA 3′ end (11). For the translational T-boxes, it has been shown that the cognate tRNA is bound by a stem II domain that is attached to a short stem I, both of which form multiple contacts to the anticodon of tRNA (12). In both cases, the structural and functional data verified that T-box-mediated regulation is achieved via the use of a multitude of recurring structural motifs and domains that collectively shape the overall RNA architecture and present the binding interfaces. Moreover, they revealed how peripheral domains provide stabilizing interactions and ensure correct orientation of the tRNA (11,12). Finally, they highlight the conformational versatility of T-boxes and prompt the elucidation of additional lineage-specific structural features, especially given the recent annotation of >23 000 T-boxes and that until now the most detailed structural and functional information has been derived mainly from studies in bacilli (27).

Several studies suggest that T-box variability could lead to the discovery of new appended RNA domains with additional modulatory functions (14,28). The recent advances highlight the flexibility and versatility of RNA structures in achieving convergent regulatory mechanisms through diverse and unique modes of tRNA recognition. It should be noted that although the detailed T-box structures have pinpointed important common conserved structural features, bioinformatics suggest that many T-boxes deviate significantly from the known patterns, suggesting a broader diversity of structural features among different T-boxes from different species that reflect their complex evolutionary history and highlight the variation in metabolic adaptation among bacteria and especially among pathogens (27–30). Current bioinformatics tools for structural prediction and annotation of putative functional T-boxes provide limited accuracy and require subsequent experimental verification (31–33).

One of the first examples of T-box structure that could not be detected with current bioinformatics tools was the *Staphylococcus aureus glyS* T-box. This T-box contains an unusual insertion domain in the terminator/antiterminator domain (termed stem Sa), and supervises the transcription of a sole *glyS* gene that encodes for glycyl-tRNA synthetase, which in turn is responsible for the aminoacylation of the five $tRNA^{Gly}$ isoacceptors present in the pathogen (15). Essentially, this special T-box controls the availability of glycine to not only ribosomal protein synthesis through glycyl-$tRNA^{Gly}$ supply (served by P1 $tRNA^{Gly}_{GCC}$ and P2 $tRNA^{Gly}_{UCC}$), but also the exoribosomal synthesis of pentaglycine peptides that stabilize the *S. aureus* cell wall. The synthesis of pentaglycine bridges utilizes non-proteinogenic (NP1 $tRNA^{Gly}_{UCC}$, NP2 $tRNA^{Gly}_{UCC}$ and NEW $tRNA^{Gly}_{UCC}$) glycyl-$tRNA^{Gly}$ isoacceptors as substrates for the family of Fem factors (factors essential for methicillin resistance; FemXAB) (34–36). It was shown previously that the *S. aureus glyS* T-box consists of stem I with low conservation compared to its bacilli counterparts and an unstructured linker sequence with no stem II, followed by a rather typical stem III, and interestingly the terminator/antiterminator domain besides the conserved T-box bulge includes the appended stem Sa insertion (42 nt), which serves as an additional selectivity and specificity node for the $tRNA^{Gly}$ isoacceptors and is present in all staphylococci. In addition, it was shown that the *S. aureusglyS* T-box responds to all five $tRNA^{Gly}$ isoacceptors, independently of the differences in the third anticodon nucleotide and with different binding affinities (15). Surprisingly, subsequent studies showed that the *S. aureus glyS* T-box can modulate transcription levels in the presence of specific mainstream antibiotics that target protein synthesis, such as tigecycline and linezolid, and it was suggested that stem Sa might have a role serving as a 'hotspot' for antibiotic-mediated modulation of transcription, similarly to what has been described for other riboswitch–antibiotic interactions (29,37,38).

The present study investigates the functional and regulatory role of stem Sa that is present in variable lengths in all known staphylococcal species, representing an evolutionarily conserved structural element. Extensive domain swap mutagenesis between *S. aureus* and *Geobacillus kaustophilus* for the generation of *glyS* T-box 'hybrids' showed that although stem Sa is important for transcriptional control, its ablation is impactful but does not lead to total loss of the *S. aureus* T-box response to tRNA binding, both *in vitro* and *in vivo*. Instead, stem Sa deletion results in deficiency in binding selectivity among those tRNA isoacceptors that serve translation (proteinogenic) and those that serve as glycine donors during cell wall formation (nonproteinogenic). On the other hand, insertion of stem Sa in the *G. kaustophilus* T-box antitermination domain results in reduced albeit significant readthrough response and confers higher tRNA binding selectivity for proteinogenic tRNAs, as it does in the staphylococcal T-box context. More interestingly, the absence of stem Sa in the *S. aureus* Δstem Sa *glyS* T-box mutant deprived the staphylococcal T-box of the ability to bind tigecycline and reverted its previously reported stimulatory effect. Instead, when the *S. aureus* Δstem Sa *glyS* T-box mutant was analyzed, tigecycline induced protections on stem

III, an essential structural feature for the T-box conformation and response. Accordingly, insertion of stem Sa in the terminator/antiterminator domain of *G. kaustophilus glyQ* T-box resulted in increased transcription levels in the presence of tigecycline *in vivo*, and subsequent chemical probing revealed that stem Sa could accommodate tigecycline-induced protections in the bacilli context, with some protection sites being identical to those observed in *S. aureus* wild-type (wt) T-box. Overall, the present study underlines the important role of species-specific T-box structural domains and emphasizes the importance of studying the variability of T-box-mediated regulation among pathogens to identify and validate new antimicrobial targets. As an example of this variability, stem Sa stands out as a lineage-specific structural feature that not only is important for the regulation of efficient staphylococcal *glyS* T-box-mediated transcription but could also serve as a species-selective druggable target by antimicrobials due to its ability to serve as a hotspot for binding of specific antibiotics.

## MATERIALS AND METHODS

### Chemicals, enzymes, plasmid vectors and bacterial strains

All T-box mutants designed for this study were synthesized by GenScript Biotech into pUC57 plasmid vectors under the endogenous promoter in the upstream region of *S. aureus glyS* T-box sequence and followed by the first 62 nt of *glyS* gene coding region. Mutant M1 contains a deletion of stem Sa, mutant M2 contains the *G. kaustophilus glyQ* T-box bearing an insertion of stem Sa in the antiterminator domain and mutant M3 contains a deletion of stem Sa and a substitution at the antiterminator cap with a 5′-GAAA-3′ tetraloop. All chemicals and antibiotics were purchased from Sigma-Aldrich or PanReac AppliChem. The primers used for primer extension analysis and *in vitro* antitermination assays were synthesized by VBC Biotech and they have been previously described (15). The primers used for the clonings for the *in vivo* experiments and for the *in vitro* transcription of T-boxes were synthesized by Eurofins Scientific (Supplementary Table S1). Restriction enzymes, DNase I, T4 DNA ligase, *Escherichia coli* RNA holoenzyme, T7 RNA polymerase, inorganic pyrophosphatase, RNase inhibitor and AMV reverse transcriptase were purchased from New England Biolabs. High-fidelity DNA polymerase was purchased from KAPA Biosystems. DMS (dimethyl sulfate) and kethoxal reagents used for chemical modification experiments were purchased from Sigma-Aldrich. Plasmid DNA was prepared using the NucleoSpin Plasmid Mini Kit and PCR products were purified by NucleoSpin Gel and PCR Clean-up Kit (Macherey-Nagel). [γ-$^{32}$P] ATP (6000 Ci/mmol) and [α-$^{32}$P] UTP (800 Ci/mmol) were purchased from Hartmann Analytic (Germany). pXS-dTomato was a gift from Karen Guillemin (Addgene plasmid # 117387; http://n2t.net/addgene:117387; RRID: Addgene_117387) (39).

### Sequence alignment and phylogenetic analysis of stem Sa

The part of the antiterminator region that includes the highly conserved T-box bulge and stem Sa from the already known *S. aureus glyS* T-box was used to retrieve homologous sequences from other staphylococcal species using standard nucleotide BLAST (blastn) (40). The algorithm parameters for blastn search were set as follows: Max target sequences 1000, Expect threshold 0.05. The results were subsequently used to perform a complete sequence alignment using Clustal Omega (41). For illustration purposes, Jalview 2.11.1.7 was used (42). Based on the alignment, a maximum likelihood method was employed for the phylogenetic analysis using MEGA11 software (43). The evolutionary history was inferred by using the maximum likelihood method and the Tamura–Nei model (44). The tree with the highest log likelihood (−198.48) is shown. Initial tree(s) for the heuristic search were obtained automatically by applying the neighbor-joining and BioNJ algorithms to a matrix of pairwise distances estimated using the Tamura–Nei model, and then selecting the topology with superior log likelihood value. The tree is drawn to scale, with branch lengths measured in the number of substitutions per site. This analysis involved 34 nucleotide sequences. All positions containing gaps and missing data were eliminated (complete deletion option). A total of 40 positions in the final dataset were included. Evolutionary analyses were conducted in MEGA11 (43).

### RNA preparation of wt and mutated *glyS* T-boxes and P1 tRNA$^{Gly}$

All T-boxes were PCR amplified with high-fidelity DNA polymerase to carry a T7 promoter leader sequence. *Staphylococcus aureus* P1 tRNA$^{Gly}_{GCC}$ and NP1 tRNA$^{Gly}_{UCC}$ were designed with a T7 promoter leader sequence and a terminal recognition site for the restriction enzyme BstNI. Linearized plasmids digested with BstNI were used as templates for subsequent *in vitro* transcription using T7 RNA polymerase. Runoff *in vitro* transcription reactions were carried out at 30°C for the T-boxes and at 37°C for the P1 tRNA$^{Gly}_{GCC}$ and NP1 tRNA$^{Gly}_{UCC}$ for 16 h in the presence of inorganic pyrophosphatase (8 U). After DNase I treatment and phenol:chloroform:isoamyl alcohol (25:24:1) extraction, transcripts were purified on 8% PAGE/8 M urea, excised after visualization under a UV lamp, and bands corresponding to the T-boxes and P1 tRNA$^{Gly}_{GCC}$ were eluted in RNA elution buffer containing 20 mM Tris–HCl (pH 7.5), 250 mM sodium acetate, 1 mM EDTA (pH 8), 0.25% SDS and 1% phenol.

### *In vitro* transcription antitermination assays

The templates for the *in vitro* transcription reactions (10 ng per reaction) were PCR fragments, including the endogenous promoter, the wt or mutated *glyS* T-box, and part of the *glyS* coding sequence (up to 62 nt). The templates were purified and sequenced prior to use. *In vitro* transcription antitermination assays were performed, as previously described (15,45). In brief, the transcription was initiated by omitting the G nucleotide, incubated at 37°C for 15 min, using [α-$^{32}$P] UTP (800 Ci/mmol; 0.25 M) to visualize the size of T-box riboswitch conformation products during transcription by 1 U of recombinant *E. coli* RNAP holoenzyme in the presence of 150 μM ApU dinucleotide (46). The ini-

tiation step is paused with heparin (20 μg/ml) and elongation of transcription is allowed by the addition of $MgCl_2$ (28 mM), KCl (86 mM) and all nucleotides in a final concentration of 5 μM each, in the presence of 300 nM cognate P1 $tRNA^{Gly}_{GCC}$ and antibiotics when necessary. Antibiotic concentration range in dose–response experiments was between 50 and 200 μM. Elongation reactions were carried out at 37°C for 5, 10 and 20 min for wt *S. aureus glyS* T-box and M1 and for 0, 10, 20 and 30 min for *G. kaustophilus glyQ* T-box and M2. Before transcription elongation induction, P1 $tRNA^{Gly}_{GCC}$ or NP1 $tRNA^{Gly}_{UCC}$ transcripts were denatured at 65°C for 5 min, in the presence of 1 mM $MgCl_2$. All transcription products were analyzed on 6% PAGE/8 M urea, after being denatured at 50°C for 5 min. Bands corresponding to transcripts in termination (T) and readthrough (RT) conformations were visualized by scanning on a phosphoimager (Fuji lm FLA 3000 platform) and were quantified using the AIDA image analyzer software (version 5.0).

### Chemical probing of M1 *glyS* T-box in the presence or absence of antibiotics

Chemical modifications were introduced in the presence of DMS and kethoxal, as previously described (15,47). M1 or M2 transcripts (20 pmol) alone or in combination with P1 $tRNA^{Gly}_{GCC}$ transcript (100 and 200 pmol) were mixed in the presence of modification buffer [70 mM HEPES–KOH, pH 7.8, 10 mM $Mg(OAc)_2$ and 270 mM KOAc] and denatured at 60°C for 10 min. After slow cooling in water bath, 100 and 200 μM of tigecycline or linezolid were added to the reactions and incubated at 25°C for 30 min and on ice for 10 min, followed by 1 mM DTT addition. The reactions were then subjected to modification by addition of DMS (1:1 dilution in 100% EtOH) or kethoxal (1:1 dilution in $H_2O$) at 30°C for 30 min. The DMS reactions were stopped by adding 0.25 M Tris acetate (pH 7.5), 0.25 M β-ME, 0.3 M sodium acetate (pH 9.2) and 0.025 mM EDTA. The kethoxal modification reactions were stopped by adding 0.3 M sodium acetate (pH 6) and 25 mM potassium borate (pH 6), followed by phenol extraction and ethanol precipitation. In M1 primer extension analysis, 2 pmol of each modified transcript was hybridized with [γ-$^{32}$P]-labeled primer TbGl1 at nucleotides 129–148 and with [γ-$^{32}$P]-labeled primer TbGl6 at nucleotides 216–238, while in M2 primer extension analysis 2 pmol of each modified transcript was hybridized with [γ-$^{32}$P]-labeled primer Gkau_PE_234–251 at nucleotides 234–251. Extension reactions were performed in the presence of 20 mM Tris acetate (pH 8.3), 10 mM $Mg(OAc)_2$, 5 mM DTT, 1 mM of each dNTP and 5 U AMV reverse transcriptase at 47°C for 1 h. Reaction products were ethanol precipitated and analyzed on 8% PAGE/8 M urea after denaturation at 80°C for 2 min. Probing analysis was visualized using a Fuji lm FLA 3000 platform and the AIDA image analyzer software (version 5.0).

### *In vivo* transcription antitermination assays

The wt and mutated *glyS* T-boxes under the control of the constitutive promoter vegII were placed before the *dTomato* gene (derivative of orange fluorescent protein) in pXS-dTomato plasmid vector (39). The P1 $tRNA^{Gly}_{GCC}$ was previously cloned in pBAD-18-Kan vector, while the NP1 $tRNA^{Gly}_{UCC}$ was cloned in the same plasmid vector in the same way, as it was described before (29). Both recombinant plasmids were used to chemically transform the *E. coli* strain M5154 [generous gift of Prof. H.D. Becker, University of Strasbourg, France; F−ΔlacZ39, λ−, trpA49(Am), recA11, relA1, rpsL150(strR), spoT1] (47). For the experiments conducted in the presence of tigecycline and linezolid, the $IC_{50}$ values used were the same as they were described before [0.176 μM (0.103 μg/ml) and 253.24 μM (85.43 μg/ml), respectively] (29). The single and double transformed strains were subsequently used to monitor the fluorescence emission of dTomato protein produced in each condition. In the cells cultured in minimal growth conditions where glycine is absent, the non-aminoacylated $tRNA^{Gly}$ binds on the T-box inducing the antitermination conformation, allowing the RNA polymerase to continue transcribing the downstream gene, i.e. *dTomato*. Overnight cultures in minimal medium (1× M9 salts, 2 mM $MgSO_4$, 0.1 mM $CaCl_2$, 0.2% glycerol supplemented with 25 μg/ml L-tryptophan) were used to inoculate cultures, starting from an $OD_{595}$ of 0.1 in minimal media under starvation (0 μg/ml) and nonstarvation conditions (100 μg/ml glycine) for 4 h, in the presence or absence of tigecycline or linezolid. 0.1% L-Arabinose was added in all the cultures to induce the expression of $tRNA^{Gly}$. After 4 h of incubation, each culture was measured at $OD_{595}$ to identify the bacterial growth and the fluorescence of dTomato was measured in Fluorostar Optima with excitation at 550 nm and absorbance at 590 nm. The fluorescence values of dTomato for each culture were divided by using the respective $OD_{595}$ values and the resulting values for each condition were further normalized to that of the wt T-box-containing strain grown in minimal medium supplemented with glycine (data not shown). The effect of endogenous tRNAs on non-specific interaction with the wt and mutant T-boxes was subtracted for each condition tested (Supplementary Figure S5). The values and error bars represent mean and standard deviation (SD); $n = 3$ biologically independent samples.

## RESULTS

### Stem Sa is a staphylococcal-specific, conserved structural element

Analysis of the terminator/antiterminator domain of known staphylococcal *glyS* T-boxes showed that stem Sa is a conserved appended domain present in all known staphylococcal species (Figure 1). Examination of representative staphylococcal genomes showed that the length of stem Sa spans between 25 and 50 nucleotides and the analysis indicates that it is the same in length and sequence between different strains within the same species. Interestingly, it includes conserved adenosines in the base of the stem (A173 and A216 in *S. aureus*; A17 and A76 of the alignment) and in positions that have been previously found protected by $tRNA^{Gly}$ [A177, A182, A196 and A198, green and blue arrows in the alignment (29)]. The phylogenetic analysis indicates that stem Sa in each species likely shared a common evolutionary origin, which later diverged into

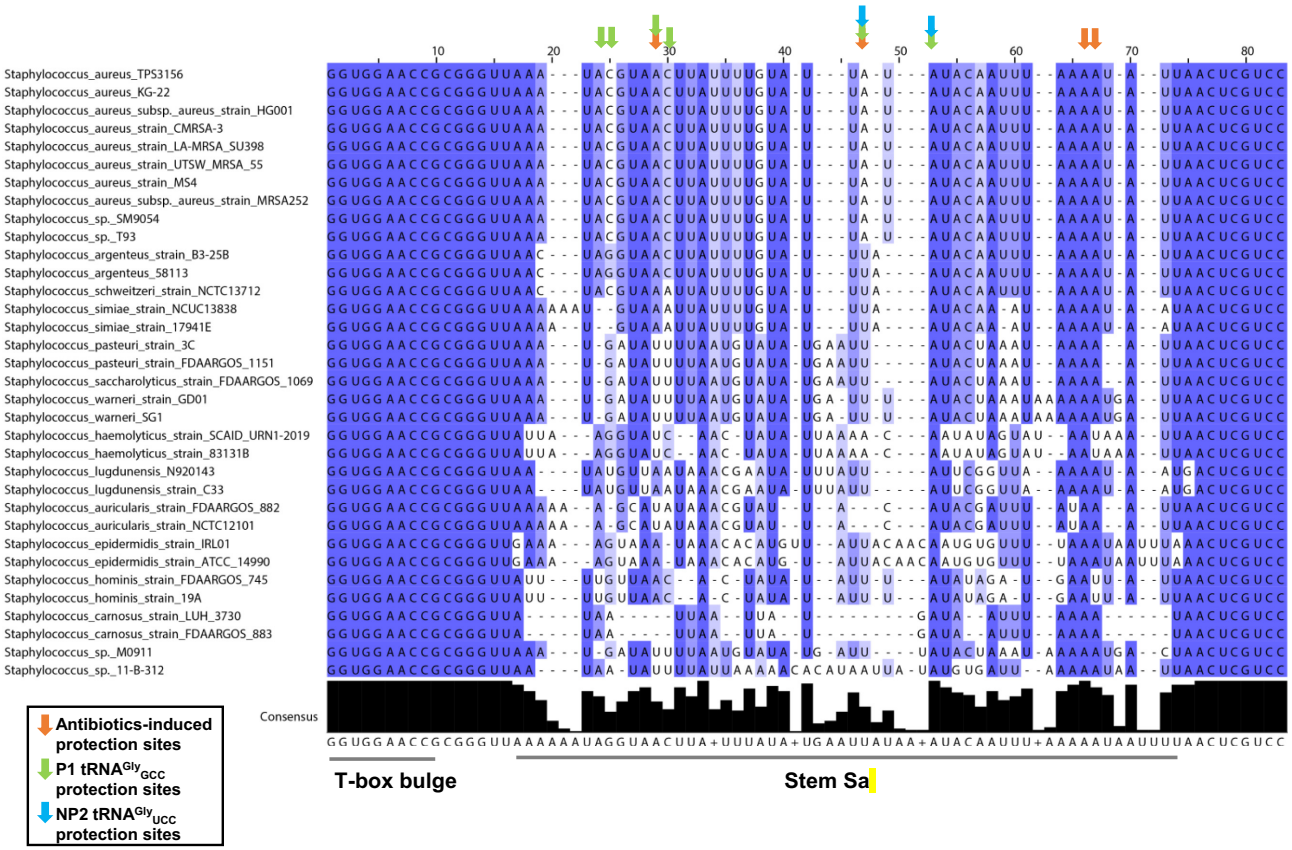


**Figure 1.** *In silico* analysis by sequence alignment of the antiterminator domain of representative staphylococcal species. For the alignment, the highly conserved nucleotides (80–100%) are indicated by dark blue color, the moderately conserved nucleotides (50–80%) are indicated with blue color, while the less conserved nucleotides (≤50%) are indicated with light blue color. The previously described antibiotic binding sites are indicated with orange arrows, the proteinogenic P1 $tRNA^{Gly}_{GCC}$ tRNA protection sites are indicated with green arrows and the nonproteinogenic NP2 $tRNA^{Gly}_{UCC}$ tRNA protection sites are indicated with blue arrows.

two major branches. The first branch primarily includes *S. aureus*-related species, and the second includes non-*S. aureus* species (Supplementary Figure S1). Additional conserved adenosines (A208 and A209) have been previously found protected by antibiotics such as tigecycline in the *S. aureus glyS* T-box (29). All attempts to identify stem Sa or stem Sa-like domains as part of terminator/antiterminator domains of T-boxes from species outside staphylococci failed, and therefore it is obvious that it represents a species-specific and evolutionary conserved structural feature of the *glyS* T-box structures. In addition, the reported interactions of both proteinogenic and nonproteinogenic tRNAs and tigecycline with stem Sa suggest that this domain may have been evolved to compensate the absence of stem II in those T-boxes. Given the differential role of each $tRNA^{Gly}$ isoacceptor in protein synthesis (proteinogenic) and cell wall formation (nonproteinogenic) through the synthesis of pentaglycine connectors, it is very likely that stem Sa has evolved to ensure the necessary conformation for proper tRNA binding and orientation. According to the recent available T-box structures, stem Sa could also ensure a more stringent transcriptional control and a platform for a tighter tRNA binding, as part of the A2 helix of antiterminator domain in both transcriptional and translational T-boxes (11,12).

## Domain swap suggests modulation of *in vitro* transcription readthrough by stem Sa

To examine whether stem Sa can alter the transcriptional response of T-boxes from species other than staphylococci, a series of mutants with cross-species swapped domains were generated between the *S. aureus glyS* T-box riboswitch and the *G. kaustophilus glyQ* T-box riboswitch (Supplementary Figure S2). Mutant M1 is a stem Sa deletion of the *S. aureus glyS* T-box (ΔStem Sa). Mutant M2 is an insertion of stem Sa in the A2 helix of the antiterminator stem of *G. kaustophilus glyQ* T-box. An additional mutant M3 contains the *S. aureus glyS* T-box, where stem Sa was replaced with a GAAA tetraloop to possibly ensure a more stable antiterminator conformation in the absence of stem Sa. All mutants were tested using standard *in vitro* antitermination assay for their ability to allow the *E. coli* RNA polymerase to 'readthrough' and transcribe the downstream gene in the presence of the uncharged cognate *S. aureus* P1 $tRNA^{Gly}_{GCC}$ (Figure 2). As control, the ability of the full-length *S. aureus glyS* T-box to induce transcription in the presence of P1 $tRNA^{Gly}_{GCC}$ was tested in a time plot, as has been previously described (15). Under the same conditions, when mutant M1 (Δstem Sa) was tested, the observed level of transcription readthrough appeared significantly lower (<50%) compared to the control T-box (Figure 2B). This

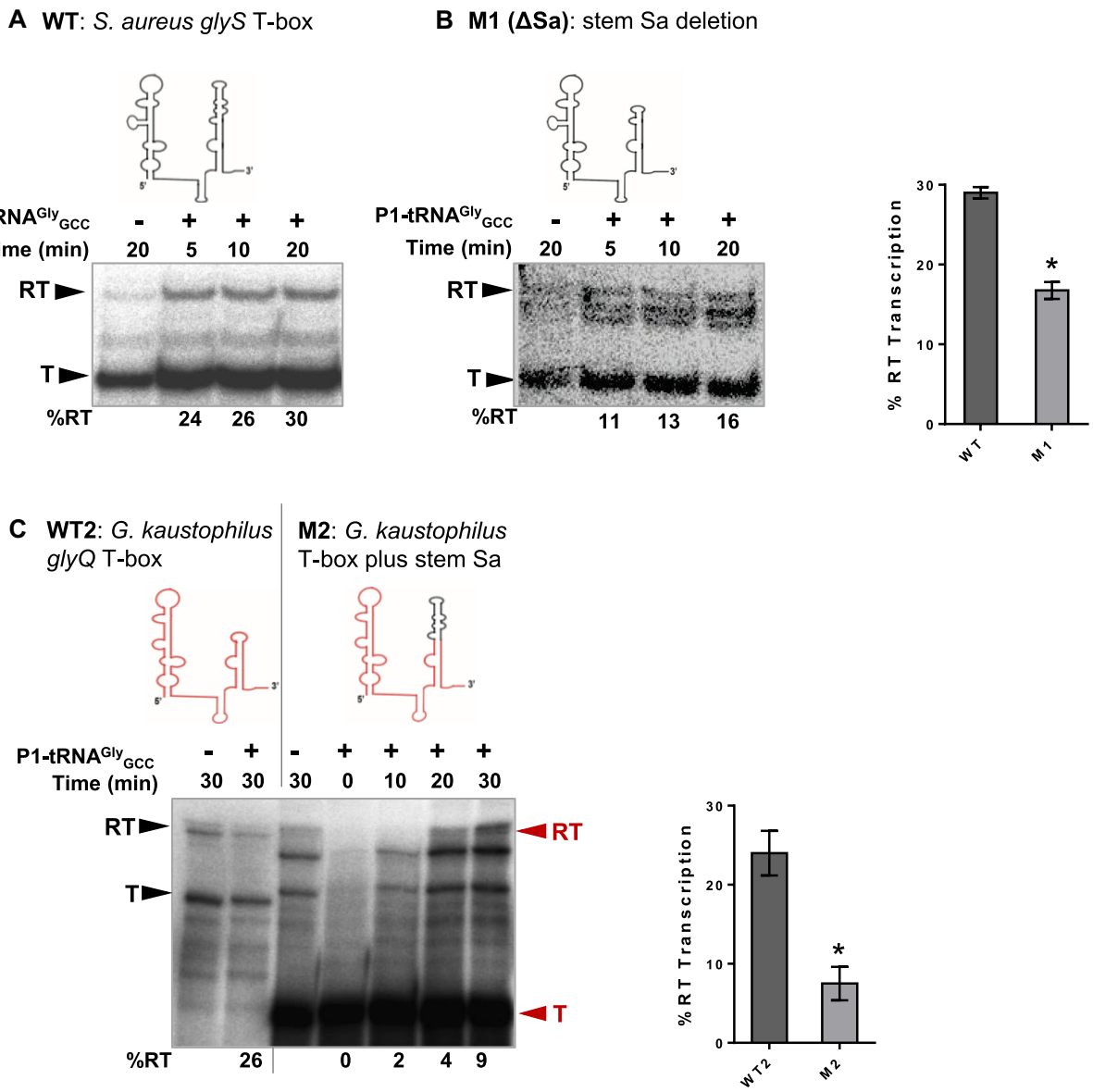


**Figure 2.** *In vitro* transcription antitermination assays of the wt and mutant T-boxes. Transcription elongation time plot of the wt *S. aureus glyS* T-box **(A)** and M1 **(B)** and wt2 and M2 **(C)** T-boxes in the absence or presence of *S. aureus* P1 tRNA$^{Gly}_{GCC}$. T and RT correspond to transcription termination and transcription readthrough, respectively. The secondary structure of each riboswitch tested is indicated on the top of readthrough assays; % readthrough transcription (represented by bars as well) is indicated in the bottom of the gels.

result suggests that although stem Sa is important for tRNA binding, its ablation is not entirely detrimental for the mutant T-box to control transcriptional readthrough (Figure 2B). However, stem Sa is important to render a fully functional *S. aureus glyS* T-box and is most likely important for better tRNA binding.

Interestingly, stem Sa insertion into the *G. kaustophilus* terminator/antiterminator domain (mutant M2) resulted in reduced transcriptional readthrough *in vitro*, when compared to the wt *G. kaustophilus glyQ* T-box, an observation that suggests that stem Sa not only is an important species-specific structural feature, but also probably interferes with the overall local conformation (Figure 2C). Moreover, it supports the notion that structural deviations from the well-characterized pattern of the bacilli T-boxes are important for a context-dependent response and highlights the role of stem Sa as an important staphylococcal-specific insertion for the overall T-box structural conformation (Figure 2C).

### Stem Sa favors tighter binding of proteinogenic tRNA$^{Gly}$ isoacceptors both *in vitro* and *in vivo*

The *S. aureus glyS* T-box can bind all five tRNA$^{Gly}$ isoacceptors (termed P1, P2, NP1, NP2 and NEW) albeit via different binding affinities that depend on their anticodon (GCC or UCC) and the identity of their elbow (Supplementary Figure S3) (15). To examine whether Δstem Sa (mutant M1) can still distinguish between proteinogenic and

nonproteinogenic $tRNA^{Gly}$ isoacceptors, we tested its ability to respond to P1 and NP1 tRNAs, *in vitro*. Interestingly, Δstem Sa decreases the ability to differentially induce transcription antitermination depending on the type of tRNA ligand. Instead, the levels of transcriptional readthrough were comparable and at the same level, regardless of the tRNA type (proteinogenic or nonproteinogenic) (Figure 3A). This result further supports the previously proposed role of stem Sa as a discriminator between proteinogenic and nonproteinogenic tRNA isoacceptors, independently of their anticodon recognition by the specifier loop codon.

To further verify the *in vitro* observations, the ability of the T-box mutants to respond and control transcription was also tested *in vivo*. An *E. coli* M5154 strain was transformed with two plasmid vectors bearing different antibiotic selection markers (for details see the 'Materials and Methods' section). The first plasmid (pXS-dTomato) was responsible for transcription of the wt T-box, or each mutant fused to the 5′UTR of the *dTomato* gene and the second plasmid (pBAD18) encoded either the P1 $tRNA^{Gly}_{GCC}$ or NP1 $tRNA^{Gly}_{UCC}$ genes. The productive binding of uncharged tRNA to the T-box affects the transcription termination or readthrough of the downstream *dTomato* gene that, upon expression, produces the RFP-derived dTomato protein with a measurable fluorescent signal (Figure 3B). The *in vivo* assays verified the *in vitro* results, showing that (i) Δstem Sa shows comparable transcription readthrough levels, independently of the tRNA isoacceptor, and (ii) although Δstem Sa exhibits a significantly reduced transcriptional readthrough response in the presence of P1 tRNA, it retains a basal regulatory ability (Figure 3C). Interestingly, in the bacilli T-box context, insertion of stem Sa in the antiterminator domain conferred mutant M2 the ability to elevate transcription in the presence of P1 tRNA compared to the transcription induced in the presence of NP1 tRNA. As observed previously *in vitro*, the *in vivo* data are supportive of a possible T-box conformation that selectively favors the binding of P1 tRNA, due to the presence of stem Sa. Finally, *in vivo* testing of mutant M3 (harbors a different stem Sa deletion where the distal loop is substituted with a stable GAAA tetraloop) also lacks the ability to distinguish between proteinogenic and nonproteinogenic tRNA isoacceptors (Supplementary Figure S4A).

### Stem Sa ablation alters the modulation pattern of T-box-mediated transcription by antibiotics

It was shown previously that tigecycline, a broad-spectrum protein synthesis inhibitor derived from tetracycline, increased transcriptional readthrough of the staphylococcal *glyS* T-box, whereas several other antibiotics inhibited T-box transcription (29). This unusual stimulatory effect of tigecycline was attributed to its binding to the specifier and apical loops of stem I and to stem Sa, which apparently favored the multivalent RNA–RNA interactions within the T-box:tRNA complex. On the other hand, antibiotics such as linezolid bound to different sites than tigecycline and suppressed transcription (29). To test the effects of stem Sa deletion on the binding of specific antibiotics and on *S. aureus glyS* T-box transcription outcome, we performed *in vitro* readthrough assays using the Δstem Sa (M1 mutant) in the presence of P1 $tRNA^{Gly}_{GCC}$ and increasing concentrations of either tigecycline or linezolid (50, 100 and 200 μM) (Figure 4A). Remarkably, in the absence of stem Sa, tigecycline exhibited a strong inhibitory effect on T-box transcription readthrough in a dose–response manner, opposite to when stem Sa was present. In contrast, linezolid exhibited inhibition of transcription in all conditions tested, regardless of the presence of stem Sa (Figure 4A). These results accentuate the role of stem Sa as a 'hotspot' for tigecycline binding. Moreover, it shows that stem Sa plays a key role in mediating the direct and differential modulation of T-box transcription by different antibiotics.

To corroborate these *in vitro* findings, we employed a previously used *in vivo* T-box readthrough assay. First, we confirmed that the addition of tigecycline stimulates the wt T-box-mediated transcription, whereas linezolid inhibits the readthrough transcription of the downstream *dTomato* gene. In agreement with the *in vitro* finding, the Δstem Sa (M1 mutant) exhibited reduced transcription in the presence of $IC_{50}$ concentration of tigecycline (0.103 μg/ml), and a similar effect was observed in the presence of $IC_{50}$ concentration of linezolid (85.43 μg/ml) (Figure 4B). These results highlight the important structural and functional role of stem Sa for either tRNA or antibiotic binding. Finally, mutant M3 showed significant inhibitory effect compared to the wt T-box in the presence of antibiotics (Supplementary Figure S4B).

### Deletion of stem Sa leads to altered antibiotic binding sites

In the next step, extensive chemical probing was performed to get insights into the alterations on tRNA and antibiotic binding caused by stem Sa deletion (Figure 5). Initially, mutant M1 transcripts were chemically modified with DMS [methylates N1 of adenine (A) and N3 of cytosine (C)] and kethoxal [methylates N1 and the exocyclic amino group (N2) of guanine (G)] in the presence or absence of the cognate P1 $tRNA^{Gly}_{GCC}$ (see the 'Materials and Methods' section). Primer extension analysis was performed using a primer that hybridizes at positions 129–148 (part of the linker and stem III sequence) to probe stem I and a primer that anneals at positions 216–238 to successfully probe the structure of stem III and the antiterminator domain (Figure 5E and Supplementary Table S1). The analysis showed tRNA protection sites on stem I at A61, A62 and G75, G77 (AG bulge). In addition, in the presence of tRNA, multiple sites of the apical loop (G82, G83 and G93) and the specifier loop (G109) were found protected. On the other hand, analysis of the terminator/antiterminator domain showed that tRNA protects A173 (distal loop of the antiterminator stem) and the highly conserved G160 and G161 of the T-box bulge, as expected. Taken together, the P1 $tRNA^{Gly}_{GCC}$ protection sites on Δstem Sa (M1 mutant) exhibited few but important differences compared to the previously reported pattern for the wt T-box, which includes A61, A62, G75, G77 and A173 (15). As expected, tigecycline also induces a different protection pattern compared to the wt T-box showing protection of positions A86 and A92 (apical loop), A103 and G109 (specifier loop), and C116 (K-turn of stem I; Figure 5A and E). Among these, only G109 pro-

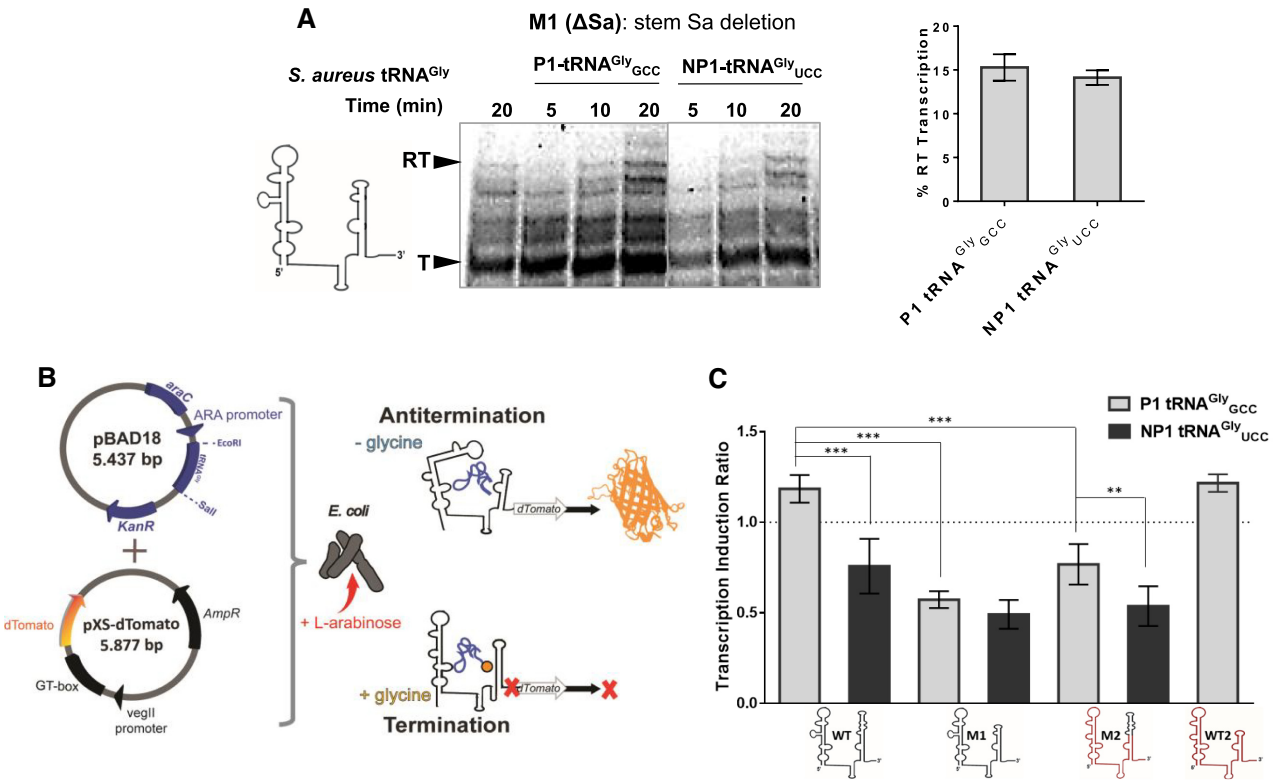


**Figure 3.** *In vitro* transcription antitermination assays of M1 T-box mutant in the presence of proteinogenic and nonproteinogenic tRNA$^{Gly}$. (**A**) *In vitro* tRNA-directed antitermination (readthrough) assay. Transcription elongation time plot of the M1 mutant T-box using two *S. aureus* tRNA$^{Gly}$ isoacceptors either proteinogenic or nonproteinogenic (P1 tRNA$^{Gly}_{GCC}$, NP1 tRNA$^{Gly}_{UCC}$). The values for the graph were extracted after analysis of representative autoradiograms (insets) as described in the 'Materials and Methods' section. Error bars represent ±SD from corresponding experiments. T and RT in black correspond to transcription termination and transcription readthrough, respectively. Reaction time is 20 min. The secondary structure of M1 T-box is indicated on the left of the readthrough assay. (**B**) Schematic representation of *in vivo glyS* T-box-mediated transcription antitermination assay of the *glyS* T-box-dependent *dTomato* expression in *E. coli*. (**C**) Relative dTomato fluorescence of wt and mutant T-boxes under glycine starvation conditions, normalized to wt T-box-containing strain grown in minimal media supplemented with glycine in the presence of P1 tRNA$^{Gly}_{GCC}$ or NP1 tRNA$^{Gly}_{UCC}$ (data not shown). The secondary structure of each riboswitch tested is indicated at the bottom of the graph. The values and error bars represent mean and SD; $n = 3$ biologically independent samples. Significance stars represent ns: $P > 0.05$, *: $P \leq 0.05$, **: $P \leq 0.01$, ***: $P \leq 0.001$ and ****: $P \leq 0.0001$.

tection has been previously observed for the wt T-box (29). In addition, tigecycline protects positions A127 and A132 of the linker and A173 and A177 of the distal loop of the antiterminator stem (Figure 5B and E). Protection of positions G60, G68, G82, G110 and A162 that were previously observed in the wt T-box was not observed for mutant M1 (29). These results clearly demonstrate that upon deletion of stem Sa, tigecycline can still bind to the mutant T-box, but its binding sites are now localized in positions that could potentially distort local RNA conformations, such as stem III.

Similar to tigecycline, the linezolid-induced protections to the M1 mutant also occur at different sites compared to the wt T-box, in the absence of tRNA. These positions include A61, A62, G75, G77, G82, G83, G89 and G93, G109 (specifier loop) and A122 (at the base of K-turn). In the antiterminator region, linezolid-induced protections were observed in A127 of the linker, A139, G142, C144 and A151 of stem III, G160 and G161 of the T-box bulge, and A173 of the distal loop of the antiterminator stem (Figure 5C and D). Only positions G93 and G109 are commonly protected between mutant M1 and the wt T-box (29). In the presence of P1 tRNA$^{Gly}_{GCC}$, linezolid protected the same sites including A61 and A62 at G75 and G77 of the stem I AG bulge, at G82, G83 and G93 of the apical loop, and at G109 of the specifier loop (Figure 5C and E). As most of these sites of T-box stem I are also protected by tRNA, it is possible that linezolid may compete with tRNA for stem I binding, and thus disrupt T-box transcription readthrough. It is also possible that the binding of antibiotics to the apical loop and AG bulge could lead to misfolding of these domains, thus creating a nonfunctional T-box riboswitch.

Finally, antibiotic-induced protections on the antiterminator may also contribute to their inhibition of T-box transcription readthrough. Both antibiotics compete with the P1 tRNA$^{Gly}_{GCC}$ for protection to A173 and the highly conserved G160 and G161 of the T-box bulge (Figure 5E). It has been shown previously (1,3,11) that the tRNA 3′-UCCA terminus base pairs with the 5′-AGGU tetranucleotide of the T-box bulge, creating an intermolecular helix that coaxially stacks with the tRNA acceptor stem and with helix A1 of the antiterminator, thus leading to the stabilization of the antiterminator and transcription readthrough. Thus, antibiotic protections to these positions would likely interfere with the intimate RNA–RNA interactions that stabilize the antitermination conformation, leading to re-

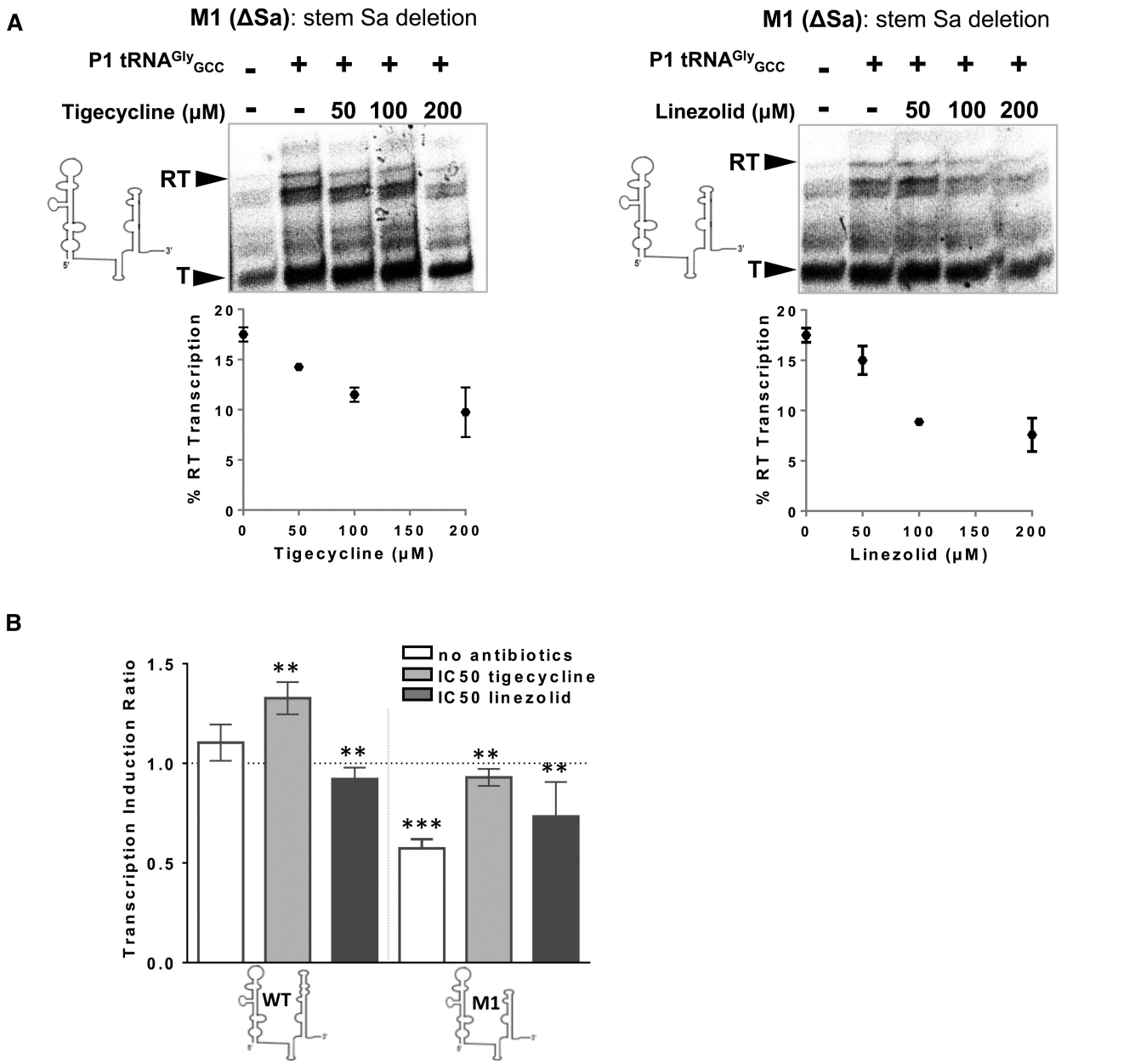


**Figure 4.** (**A**) Dose–response graphs showing the effect of increasing concentration of tigecycline and linezolid on the M1 T-box readthrough reaction, *in vitro*, in the presence of P1 tRNA$^{Gly}_{GCC}$. The values for the curves were extracted after analysis of representative autoradiograms, as described in the 'Materials and Methods' section. All reactions were performed twice in duplicates and error bars represent ±SD from the corresponding experiments. T and RT correspond to transcription termination and transcription readthrough, respectively. The secondary structure of the M1 T-box is indicated at the left of readthrough. Reaction time is 20 min. (**B**) Relative dTomato fluorescence of wt and T-box mutants under glycine starvation conditions, normalized to the wt T-box-containing strain grown in minimal media and supplemented with glycine (data not shown). Relative dTomato fluorescence of wt and T-box mutants was measured both in the presence and in the absence of $IC_{50}$ concentrations of linezolid and tigecycline. The secondary structure of each riboswitch tested is indicated at the bottom of the graph. The values and error bars represent mean and SD; $n = 3$ biologically independent samples. Significance stars represent ns: $P > 0.05$, *: $P \leq 0.05$, **: $P \leq 0.01$, ***: $P \leq 0.001$ and ****: $P \leq 0.0001$.

duced transcription readthrough of the M1 mutant. Of note, tigecycline shares with linezolid the binding position A127, while additional protection by tigecycline at A132 of the linker was detected (Figure 5E). These interactions could affect the flexibility of the linker, leading to a less flexible structure that may not allow the base of stem III and its flanking purines to interact and stabilize the antiterminator.

### Insertion of stem Sa in the *G. kaustophilus* T-box context induces binding of tigecycline

It was shown previously that grafting stem Sa onto the bacilli T-box scaffold (mutant M2) reduced the T-box-mediated transcription *in vitro* (Figure 2C). Surprisingly, when the same mutant was in the presence of $IC_{50}$ concentration of tigecycline, an increased transcription level was

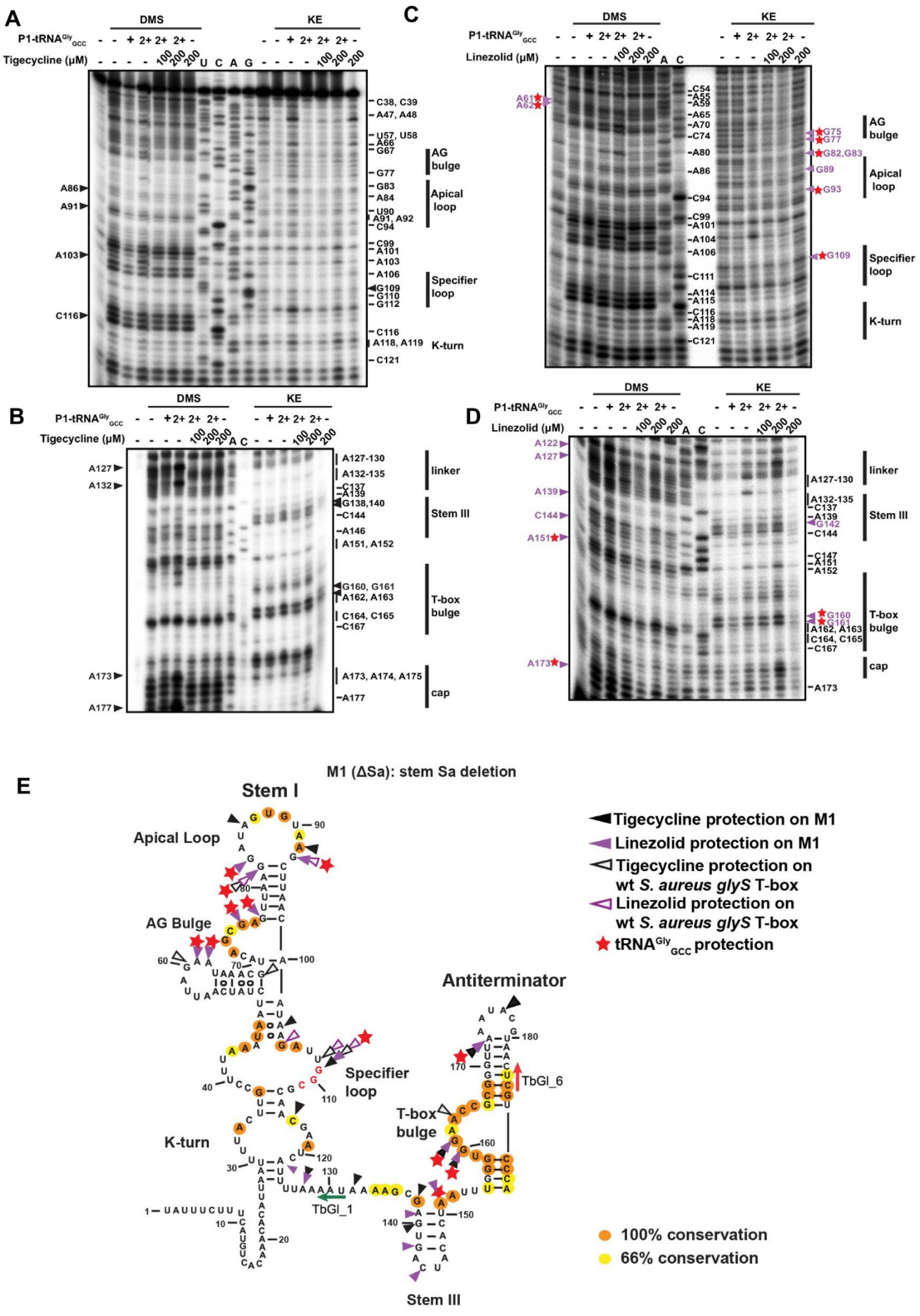


**Figure 5.** Chemical probing analysis of M1 T-box stem I in complex with the P1 tRNA$^{Gly}_{GCC}$, tigecycline and linezolid. Chemical probing of M1 mutant (20 pmol) in the presence or the absence of P1 tRNA$^{Gly}_{GCC}$ (+ and 2+ refer to 100 and 200 pmol, respectively) and/or increasing concentrations of **(A, B)** tigecycline and **(C, D)** linezolid. Black arrows indicate tigecycline-induced protection sites and magenta arrows indicate linezolid-induced protection sites on M1. Red stars indicate P1 tRNA$^{Gly}_{GCC}$ induced protection sites on M1. (**E**) Illustration of M1 secondary structure. The protection sites of P1 tRNA$^{Gly}_{GCC}$, tigecycline and linezolid on M1 are shown with red stars, black arrows and magenta arrows, respectively, while the protection sites induced by tigecycline and linezolid on the wt *S. aureus glyS* T-box are indicated with open black outlined arrows and open magenta outlined arrows, respectively. TbGl1 primer (green arrow) was used for stem I primer extension analysis, while TbGl6 (red arrow) primer was used for terminator/antiterminator stem primer extension analysis. The 100% conserved nucleotides are labeled in orange, while the 66% conserved nucleotides are labeled in yellow.

observed compared to the wt *G. kaustophilus glyQ* T-box (Figure 6A). This result is consistent with previous observations for the *S. aureus glyS* T-box, where tigecycline binds on stem Sa and stabilizes tRNA binding to increase transcription readthrough both *in vitro* and *in vivo* (29).

To elucidate this interesting observation, we probed the protection sites of tigecycline on M2 mutant, using chemical probing analysis on the terminator/antiterminator region in the absence or presence of P1 $tRNA^{Gly}_{GCC}$ (for details see the 'Materials and Methods' section). Primer extension analysis was performed using a primer that hybridizes at positions 234–251 (Gkau_PE_234–251) that covers probing of the inserted stem Sa. Interestingly, the analysis verified some tigecycline-induced protection sites on stem Sa at positions C181, G182, A185 and C186, of which A185 (the latter corresponds to A182 of *S. aureus glyS* T-box) was also found previously protected by tigecycline on the stem Sa of the wt *S. aureus glyS* T-box (Figure 6B and C) (29). In addition, tigecycline induced protections on G162, A163 and A164 of the T-box bulge. Of note, A163 of mutant M2 was previously reported to be also protected by tigecycline in *S. aureus glyS* T-box (corresponds to *S. aureus* A162) (Figure 6B and C). Moreover, in the presence of tigecycline, additional positions of the A2 helix (G169, G170), stem III (G144) and the linker (A119, C125, A128 and A129) were also found protected (Figure 6B). Collectively, our results show that upon insertion on *G. kaustophilus* T-box context, stem Sa preserves its ability to act as a hotspot for tigecycline binding, which also explains the elevated *in vivo* transcription readthrough that was observed.

The main protection sites that are induced in the presence of antibiotics were mapped on the available *Bacillus subtilis glyQS* T-box structure in complex with its cognate tRNA (PDB: 6POM). The analysis indicated that the apical loop, the specifier loop and the antiterminator stem are important putative antibiotic binding sites that could also modulate RNA–RNA interactions and therefore could affect the transcription regulation ability of the T-box not only via direct binding but also due to conformational changes that are induced by either the tRNA ligands or the antibiotics, or both (Figure 7). Finally, the molecular structure and precise mechanism of stem Sa in the staphylococci *glyS* T-boxes remain to be elucidated, by its complex structure with either P or NP $tRNA^{Gly}$ isoacceptors.

## DISCUSSION

Although T-box riboswitches have been described almost 30 years ago, the mechanism by which they can sense charged or uncharged tRNAs has been elucidated only recently (11,12,48). Most of the knowledge on how T-boxes sense amino acid availability in different environmental niches comes mainly from mutational analyses in bacilli counterparts. However, broader phylogenetic analyses suggest that T-boxes, especially among pathogens, exhibit a remarkable variability in length and structural idiosyncrasies that, although cannot be directly linked to co-evolution with the tRNA ligands, is concomitant with the function of specific tRNA isoacceptors (14,28,29).

The *S. aureus glyS* T-box riboswitch is a distinct example of an RNA transcription attenuator that synchronizes two metabolically related pathways: protein synthesis and cell wall formation. The existence of a staphylococci-specific stem Sa embedded in the terminator/antiterminator domain provides a unique structural feature for tRNA discrimination and coordinates regulation of both pathways (15). Similar staphylococci-specific domains have been also recently described for the *S. aureus* MET-T-box riboswitch that accommodates three additional stem loops within its linker region. In both cases, novel RNA structural features have been acquired and retained through evolution for adaptation to specific metabolic environments or for binding tRNA ligands of specific characteristics (49). Based on the available structural information from bacilli and our findings, we propose that stem Sa is an evolutionary conserved feature that could have co-evolved with the *glyS* T-box to optimize tRNA binding as part of the A2 helix of the antiterminator domain. Stem Sa may enhance tRNA binding by making additional contacts or confer tRNA binding specificity among different tRNA isoacceptors. Its conservation in all known staphylococci species suggests a potential role in coordinating glycine utilization by the ribosomal translational machinery and by the FEM factors that synthesize the pentaglycine bridges for cell wall stabilization (50,51).

Interestingly, several widely used antibiotics in clinical settings have the ability to bind on stem Sa, thus contributing to a direct modulation of T-box-mediated transcription (29). The present study shows that stem Sa not only acts as a 'hotspot' of antibiotic binding, but its presence in the context of 'textbook' T-boxes (like *G. kaustophilus*) can actually alter their regulatory behavior and character. Moreover, the absence of stem Sa redirects antibiotic-induced protections onto other T-box regions that are crucial for the conformation of the terminator/antiterminator domain, leading to the inability of T-box to induce transcription readthrough. Moreover, antibiotics that have been previously shown to attenuate T-box transcription, such as linezolid, showed different binding sites, particularly on stem I.

One of the main aims of this study was to elucidate to what extent and how stem Sa is involved in the T-box-mediated transcription control. The mutagenic analysis showed that stem Sa is required for a fully functional *S. aureus glyS* T-box and stem Sa deletion or stem Sa insertion in *G. kaustophilus glyQ* T-box leads to reduction of the transcription both *in vitro* and *in vivo.* Minor structural differences could also contribute, arising from a shorter or longer stem III in *S. aureus* and *G. kaustophilus*, respectively, a domain that is essential for the overall local conformation of the terminator/antiterminator domain and serves as an extended latch around the tRNA's 3′ end to fasten and stiffen the entire discriminator around the T-box bulge (11).

T-box riboswitches act as molecular rulers and have flexible and segmented RNA structures able to inspect the overall shape of an incoming tRNA ligand and brace the elbow of the tRNA, to make orthogonal distance measurements (21,52). Extensive studies have been focused on the importance of tRNA elbow recognition by T-boxes, which ensures that the incoming tRNA molecules conform to the expected L-shape and present a well-formed flat surface at the elbow (8,17,21). Indeed, immediately after the initial contact between the tRNA anticodon and T-box-specifier codon is

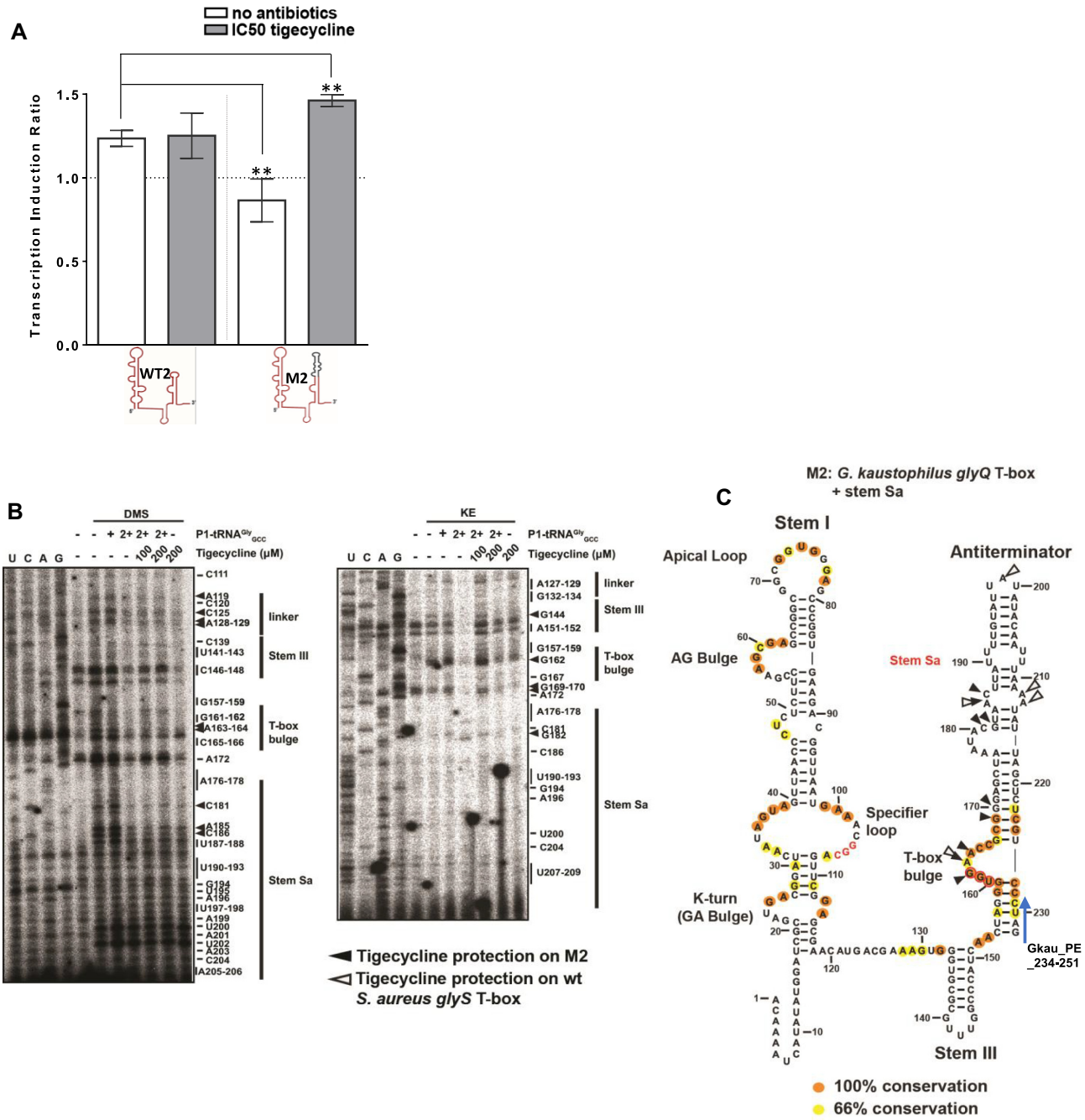


**Figure 6.** (**A**) Relative dTomato fluorescence of wt G. *kaustophilus glyQ* T-box and mutant M2 under glycine starvation conditions, normalized to the wt T-box-containing strain grown in minimal media and supplemented with glycine (data not shown). Relative dTomato fluorescence of wt and M2 was measured both in the presence and in the absence of $IC_{50}$ concentrations of tigecycline. The secondary structure of each riboswitch tested is indicated at the bottom of the graph. The values and error bars represent mean and SD; $n = 3$ biologically independent samples. Significance stars represent ns: $P > 0.05$, *: $P \leq 0.05$, **: $P \leq 0.01$, ***: $P \leq 0.001$ and ****: $P \leq 0.0001$ (**B**) Chemical probing analysis of M2 T-box stem I in complex with the P1 $tRNA^{Gly}_{GCC}$ and tigecycline. Chemical probing of M2 mutant (20 pmol) in the presence or the absence of P1 $tRNA^{Gly}_{GCC}$ (+ and 2+ refer to 100 and 200 pmol, respectively) and/or increasing concentrations of tigecycline. Black arrows indicate tigecycline binding sites on M2. (**C**) Illustration of M2 secondary structure. The protection sites induced by tigecycline on M2 are shown with black arrows, while the protection sites induced by tigecycline on the wt *S. aureus glyS* T-box are shown with open black outlined arrows. Gkau_PE_234–251 primer (blue arrow) was used for terminator/antiterminator stem primer extension analysis. The 100% conserved nucleotides are labeled in orange, while the 66% conserved nucleotides are labeled in yellow.

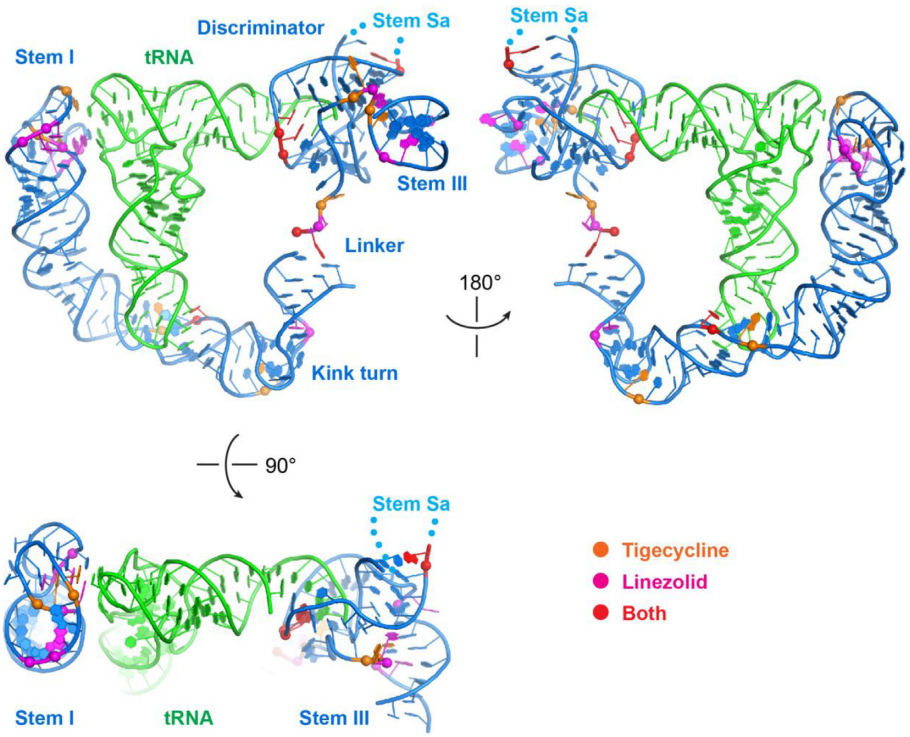


**Figure 7.** Front (upper left), back (upper right) and top (below) views of a 3D computational model of the full-length *B. subtilis glyQS* T-box riboswitch in complex with $tRNA^{Gly}$ (PDB: 6POM) with the proposed induced protections by tigecycline (orange), linezolid (magenta) and both (red) found in M1.

established, additional interactions take place to promote binding (by 2–20-fold) and to prevent premature tRNA release (18). There are many examples in nature where the tRNA elbow participates in important interactions during ribosomal translation, modification of tRNA, maturation by RNase P, etc. (21,53,54). Even viruses hijack tRNA binding molecules from the host by mimicking the tRNA structure (55,56). Similarly, stem Sa interacts with specific nucleotides of the T-loop of all $tRNA^{Gly}$ isoacceptors from *S. aureus* (A196, A198), while additional interacting points are observed with P1 $tRNA^{Gly}_{GCC}$ (A177, C178, A182, C183) to form a tight and functional T-box:tRNA complex (15). Interestingly, this study shows that stem I interfaces with each tRNA isoacceptor including the specifier and apical loops are largely similar and nondiscriminative for proteinogenic or nonproteinogenic tRNAs. However, in the presence of stem Sa, the *glyS* T-box was able to contribute in the discrimination among the $tRNA^{Gly}$ isoacceptors based on both the *in vitro* and *in vivo* transcription levels, an observation supported by the fact that stem Sa deletion leads to reduced transcription independently of the binding of either proteinogenic or nonproteinogenic $tRNA^{Gly}$. Therefore, although the differences in the tRNA anticodon triplet that defines specificity through base pairing with the codon-like triplet of the specifier loop are important for tRNA binding, the presence of stem Sa could represent an additional auxiliary discriminator factor. The most intriguing observation was that the addition of stem Sa conferred the *G. kaustophilus glyQ* T-box with the ability to discriminate P1 over NP1 $tRNA^{Gly}$, *in vivo*. Taken together, both the *in vitro* and *in vivo* results highlight the important role of stem Sa in the differential binding of tRNA isoacceptors and its contribution to the staphylococcal *glyS* T-box-mediated transcription of the sole glycyl-tRNA synthetase, which in turn synchronizes the supply of glycine for two different albeit related metabolic pathways.

The important role of stem Sa in the binding and response to two protein synthesis inhibitors, tigecycline and linezolid, on the T-box-mediated transcription was further elucidated. Although tigecycline has been previously demonstrated to increase *S. aureus glyS* T-box-mediated transcription by strong binding on stem Sa, upon stem Sa deletion tigecycline exhibited an inhibitory effect (29). In contrast, linezolid consistently exhibited an inhibitory effect. Further, when stem Sa was absent, both inhibitors appeared to bind to the interdomain linker and stem III, whereas only linezolid seemed to compete with the tRNA for binding on the same positions of stem I. In addition, tigecycline was found to bind the linker sequence and the cap of the antiterminator stem, while linezolid was bound at the base of stem III. Stem III, which is a ubiquitous structural element present in all known T-boxes, includes also primary antibiotic-induced protection sites that could be responsible for the inhibition of the T-box transcription readthrough. The recent structural analysis of the *glyQ* T-box riboswitch from *G. kaustophilus* showed that there is an interplay between stem III and its flanking purines with the adjoining antiterminator stem that creates a unit that discriminates uncharged against charged tRNAs, permitting the RNA polymerase to readthrough and transcribe the regulated genes. Moreover, when these conserved flanking purines of stem III were removed, tRNA binding was

abolished (11). Because of this crucial function of stem III in stabilizing the antiterminator, the antibiotic-induced protections on stem III could destabilize the antiterminator conformation, thus explaining the reduction of transcription readthrough that was observed. Moreover, substitutions of the conserved flanking purines of stem III, such as A151, abolished tRNA binding and therefore the protection of linezolid in this position reported herein could additionally account for linezolid's inhibitory effect (11). Tigecycline shares A127 in the linker as a common protection position with linezolid and an additional protection at A132 of the linker by tigecycline was detected. These interactions could affect the structure or flexibility of this region and inhibit the proper tRNA positioning, thus leading the T-box riboswitch to stabilize the termination conformation. These intervening structures that link the stem I and antiterminator domains might further function to modulate the kinetics of the transcribing RNA polymerase, extending the time frame for the cognate tRNA to engage the cotranscriptionally folding T-box stem I and to progress toward binding equilibrium (57). Indeed, bacilli *glyQS* stem III was shown to contain a prominent transcriptional pause site (58). Therefore, tigecycline and linezolid binding near these linker sites might impair the entry into or exit from the pause state, thus adversely impacting T-box function via effects on RNA polymerase kinetics or cotranscriptional folding. Taken together, our data suggest that *Staphylococcus* stem Sa is a functionally important lineage-specific structural feature that upon deletion affects not only tRNA binding but also T-box interactions with and responses to mainstream antibiotics.

Additionally, when stem Sa was inserted in the *G. kaustophilus glyQ* T-box, tigecycline induced protection on several known and new sites, an observation that explains the elevated *in vivo* transcription readthrough by mutant M2 in the presence of tigecycline (29). Given the evolutionary conservation of specific nucleotides connecting stem III, the T-box bulge and stem Sa, as a response to tRNA binding the stem Sa insertion might disrupt local structures that are important. The swap between the terminator and antiterminator domains thus involves elements important for both the T-box structure and the tRNA binding. As such, the protections observed by chemical probing may reflect on the architecture of discrete conformations arising from the stimulatory effects of the charged or uncharged tRNA ligands, which *in vivo* could also be intensified from possible competition with translation factors, such as EF-Tu, rather than on direct interactions with the tRNA or the antibiotics. This could also represent an additional explanation regarding the observation that stem Sa insertion within the bacilli T-box context results in a behavior similar to the *S. aureus* T-box, and the possible induction of additional effects due to the absence of an evolutionary link between the individual domains. Overall, the observations point toward the role of stem Sa as a key player in these dynamic interactions and its crucial contribution for a proper structural fit of the tRNA ligand on staphylococcal *glyS* T-boxes. Moreover, it confirms that species-specific structures in T-box riboswitches that have emerged through evolution are related to specific contexts of tRNA isoacceptors.

In general, bacterial RNA regulatory elements such as T-box riboswitches are increasingly identified as potential antimicrobial drug targets, as they participate in the regulation of multiple metabolic pathways (59–61). The available structural information that largely defines the T-box:tRNA complexes, along with the observed response of riboswitches to mainstream antibiotics, invites deeper investigations of the structure and function of T-boxes as promising and species-specific molecular targets. Additional and very recent studies reported the design of synthetic compounds that can specifically target and disturb the codon–anticodon interaction at the specifier loops of different T-box types or the T-box antiterminator conformation causing the inhibition of the T-box regulatory mechanism (62,63). As stem Sa mediates the binding and action of protein synthesis inhibitors, it could be considered a promising and staphylococcal-specific drug target. In conclusion, the variability and diversity of species-specific T-boxes could be further harnessed for the design of new and efficient antibiotics and could shed light on the evolution of RNA-mediated gene expression. These insights may also inform the development and optimization of T-box-targeted antibiotics to treat drug-resistant bacteria such as methicillin-resistant *S. aureus*.

## DATA AVAILABILITY

All materials and data are available upon request.

## SUPPLEMENTARY DATA

Supplementary Data are available at NAR Online.

## ACKNOWLEDGEMENTS

The research project was supported by the Hellenic Foundation for Research and Innovation (H.F.R.I.) under the "1st Call for H.F.R.I. Research Projects to support Faculty Members & Researchers and the Procurement of High-and the procurement of high-cost research equipment grant" (Project Number: 739) to CS. This research was supported by Grant 81344 from the Research Committee of the University of Patras via C. CARATHEODORI program to VS. AK is a recipient of a fellowship from the Grant "81344" from the Research Committee of the University of Patras via "C. CARATHEODORI" program.

## FUNDING

Hellenic Foundation for Research and Innovation [HFRI-FM17-739 to C.S.]; University of Patras [81344 to V.S. and A.K.]; National Institute of Diabetes and Digestive and Kidney Diseases [ZIADK075136 to J.Z.]; National Institutes of Health [to J.Z.]. Funding for open access charge: Hellenic Foundation for Research and Innovation [HFRI-FM17-739].
*Conflict of interest statement.* None declared.

## REFERENCES

1. Grundy,F.J. and Henkin,T.M. (1993) tRNA as a positive regulator of transcription antitermination in *B. subtilis*. *Cell*, **74**, 475–482.

2. Henkin,T.M. (2014) The T box riboswitch: a novel regulatory RNA that utilizes tRNA as its ligand. *Biochim. Biophys. Acta: Gene Regul. Mech.*, **1839**, 959–963.
3. Gutierrez-Preciado,A., Henkin,T.M., Grundy,F.J., Yanofsky,C. and Merino,E. (2009) Biochemical features and functional implications of the RNA-based T-box regulatory mechanism. *Microbiol. Mol. Biol. Rev.*, **73**, 36–61.
4. Henkin,T.M. (2008) Riboswitch RNAs: using RNA to sense cellular metabolism. *Genes Dev.*, **22**, 3383–3390.
5. Zhang,J. and Ferré-D'Amaré,A.R. (2015) Structure and mechanism of the T-box riboswitches. *Wiley Interdiscip. Rev. RNA*, **6**, 419–433.
6. Sherwood,A.V., Grundy,F.J. and Henkin,T.M. (2015) T box riboswitches in Actinobacteria: translational regulation via novel tRNA interactions. *Proc. Natl Acad. Sci. U.S.A.*, **112**, 1113–1118.
7. Grigg,J.C., Chen,Y., Grundy,F.J., Henkin,T.M., Pollack,L. and Ke,A. (2013) T box RNA decodes both the information content and geometry of tRNA to affect gene expression. *Proc. Natl Acad. Sci. U.S.A.*, **110**, 7240–7245.
8. Zhang,J. and Ferré-D'Amaré,A.R. (2013) Co-crystal structure of a T-box riboswitch stem I domain in complex with its cognate tRNA. *Nature*, **500**, 363–366.
9. Kreuzer,K.D. and Henkin,T.M. (2018) The T-box riboswitch: tRNA as an effector to modulate gene regulation. *Microbiol. Spectr.*, **6**, 89–100.
10. Zhang,J. and Ferré-D'Amaré,A.R. (2014) Direct evaluation of tRNA aminoacylation status by the T-box riboswitch using tRNA–mRNA stacking and steric readout. *Mol. Cell*, **55**, 148–155.
11. Li,S., Su,Z., Lehmann,J., Stamatopoulou,V., Giarimoglou,N., Henderson,F.E., Fan,L., Pintilie,G.D., Zhang,K., Chen,M. *et al.* (2019) Structural basis of amino acid surveillance by higher-order tRNA–mRNA interactions. *Nat. Struct. Mol. Biol.*, **26**, 1094–1105.
12. Suddala,K.C. and Zhang,J. (2019) High-affinity recognition of specific tRNAs by an mRNA anticodon-binding groove. *Nat. Struct. Mol. Biol.*, **26**, 1114–1122.
13. Raina,M. and Ibba,M. (2014) tRNAs as regulators of biological processes. *Front. Genet.*, **5**, 171.
14. Saad,N.Y., Stamatopoulou,V., Brayé,M., Drainas,D., Stathopoulos,C. and Becker,H.D. (2013) Two-codon T-box riboswitch binding two tRNAs. *Proc. Natl Acad. Sci. U.S.A.*, **110**, 12756–12761.
15. Apostolidi,M., Saad,N.Y., Drainas,D., Pournaras,S., Becker,H.D. and Stathopoulos,C. (2015) A glyS T-box riboswitch with species-specific structural features responding to both proteinogenic and nonproteinogenic $tRNA^{Gly}$ isoacceptors. *RNA*, **21**, 1790–1806.
16. Skeparnias,I. and Zhang,J. (2021) Cooperativity and interdependency between RNA structure and RNA–RNA interactions. *Noncoding RNA*, **7**, 81.
17. Lehmann,J., Jossinet,F. and Gautheret,D. (2013) A universal RNA structural motif docking the elbow of tRNA in the ribosome, RNAse P and T-box leaders. *Nucleic Acids Res.*, **41**, 5494–5502.
18. Zhang,J. (2020) Unboxing the T-box riboswitches—a glimpse into multivalent and multimodal RNA–RNA interactions. *Wiley Interdiscip. Rev. RNA*, **11**, e1600.
19. Jentzsch,F. and Hines,J.V (2012) Interfacing medicinal chemistry with structural bioinformatics: implications for T box riboswitch RNA drug discovery. *BMC Bioinformatics*, **13**, S5.
20. Armstrong,I., Aldhumani,A.H., Schopis,J.L., Fang,F., Parsons,E., Zeng,C., Hossain,M.I., Bergmeier,S.C. and Hines,J.V. (2020) RNA drug discovery: conformational restriction enhances specific modulation of the T-box riboswitch function. *Bioorg. Med. Chem.*, **28**, 115696.
21. Zhang,J. and Ferré-D'Amaré,A. (2016) The tRNA elbow in structure, recognition and evolution. *Life*, **6**, 3.
22. Zhang,J. and Ferré-DAmaré,A. (2016) Trying on tRNA for size: RNase P and the T-box riboswitch as molecular rulers. *Biomolecules*, **6**, 18.
23. Gerdeman,M.S., Henkin,T.M. and Hines,J.V. (2003) Solution structure of the *Bacillus subtilis* T-box antiterminator RNA: seven nucleotide bulge characterized by stacking and flexibility. *J. Mol. Biol.*, **326**, 189–201.
24. Yousef,M.R., Grundy,F.J., Henkin,T.M. and Karn,J. (2005) Structural transitions induced by the interaction between tRNA Gly and the *Bacillus subtilis* glyQS T box leader RNA. *J. Mol. Biol.*, **349**, 273–287.
25. Fauzi,H., Agyeman,A. and Hines,J.V. (2009) T box transcription antitermination riboswitch: influence of nucleotide sequence and orientation on tRNA binding by the antiterminator element. *Biochim. Biophys. Acta: Gene Regul. Mech.*, **1789**, 185–191.
26. Sherwood,A.V., Frandsen,J.K., Grundy,F.J. and Henkin,T.M. (2018) New tRNA contacts facilitate ligand binding in a *Mycobacteriumsmegmatis* T box riboswitch. *Proc. Natl Acad. Sci. U.S.A.*, **115**, 3894–3899.
27. Marchand,J.A., Pierson Smela,M.D., Jordan,T.H.H., Narasimhan,K. and Church,G.M. (2021) TBDB: a database of structurally annotated T-box riboswitch:tRNA pairs. *Nucleic Acids Res.*, **49**, D229–D235.
28. Vitreschak,A.G., Mironov,A.A., Lyubetsky,V.A. and Gelfand,M.S. (2008) Comparative genomic analysis of T-box regulatory systems in bacteria. *RNA*, **14**, 717–735.
29. Stamatopoulou,V., Apostolidi,M., Li,S., Lamprinou,K., Papakyriakou,A., Zhang,J. and Stathopoulos,C. (2017) Direct modulation of T-box riboswitch-controlled transcription by protein synthesis inhibitors. *Nucleic Acids Res.*, **45**, 10242–10258.
30. Wels,M., Kormelink,T., Kleerebezem,M., Siezen,R.J. and Francke,C. (2008) An *in silico* analysis of T-box regulated genes and T-box evolution in prokaryotes, with emphasis on prediction of substrate specificity of transporters. *BMC Genomics*, **9**, 330.
31. Butcher,S.E. and Pyle,A.M. (2011) The molecular interactions that stabilize RNA tertiary structure: RNA motifs, patterns, and networks. *Acc. Chem. Res.*, **44**, 1302–1311.
32. Miao,Z., Adamiak,R.W., Antczak,M., Boniecki,M.J., Bujnicki,J., Chen,S.-J., Cheng,C.Y., Cheng,Y., Chou,F.-C., Das,R. *et al.* (2020) RNA-Puzzles Round IV: 3D structure predictions of four ribozymes and two aptamers. *RNA*, **26**, 982–995.
33. Li,B., Cao,Y., Westhof,E. and Miao,Z. (2020) Advances in RNA 3D structure modeling using experimental data. *Front. Genet.*, **11**, 574485.
34. Giannouli,S., Labrou,M., Kyritsis,A., Ikonomidis,A., Pournaras,S., Stathopoulos,C. and Tsakris,A. (2010) Detection of mutations in the FemXAB protein family in oxacillin-susceptible mecA-positive *Staphylococcus aureus* clinical isolates. *J. Antimicrob. Chemother.*, **65**, 626–633.
35. Giannouli,S., Kyritsis,A., Malissovas,N., Becker,H.D. and Stathopoulos,C. (2009) On the role of an unusual $tRNA^{Gly}$ isoacceptor in *Staphylococcus aureus*. *Biochimie*, **91**, 344–351.
36. Villet,R., Fonvielle,M., Busca,P., Chemama,M., Maillard,A.P., Hugonnet,J.-E., Dubost,L., Marie,A., Josseaume,N., Mesnage,S. *et al.* (2007) Idiosyncratic features in tRNAs participating in bacterial cell wall synthesis. *Nucleic Acids Res.*, **35**, 6870–6883.
37. Anupam,R., Denapoli,L., Muchenditsi,A. and Hines,J.V. (2008) Identification of neomycin B-binding site in T box antiterminator model RNA. *Bioorg. Med. Chem.*, **16**, 4466–4470.
38. Orac,C.M., Zhou,S., Means,J.A., Boehm,D., Bergmeier,S.C. and Hines,J.V. (2011) Synthesis and stereospecificity of 4,5-disubstituted oxazolidinone ligands binding to T-box riboswitch RNA. *J. Med. Chem.*, **54**, 6786–6795.
39. Wiles,T.J., Wall,E.S., Schlomann,B.H., Hay,E.A., Parthasarathy,R. and Guillemin,K. (2018) Modernized tools for streamlined genetic manipulation and comparative study of wild and diverse proteobacterial lineages. *mBio*, **9**, e01877-18.
40. Altschul,S.F., Gish,W., Miller,W., Myers,E.W. and Lipman,D.J. (1990) Basic local alignment search tool. *J. Mol. Biol.*, **215**, 403–410.
41. Goujon,M., McWilliam,H., Li,W., Valentin,F., Squizzato,S., Paern,J. and Lopez,R. (2010) A new bioinformatics analysis tools framework at EMBL-EBI. *Nucleic Acids Res.*, **38**, W695–W699.
42. Waterhouse,A.M., Procter,J.B., Martin,D.M.A., Clamp,M. and Barton,G.J. (2009) Jalview Version 2—a multiple sequence alignment editor and analysis workbench. *Bioinformatics*, **25**, 1189–1191.
43. Tamura,K., Stecher,G. and Kumar,S. (2021) MEGA11: Molecular Evolutionary Genetics Analysis Version 11. *Mol. Biol. Evol.*, **38**, 3022–3027.
44. Tamura,K. and Nei,M. (1993) Estimation of the number of nucleotide substitutions in the control region of mitochondrial DNA in humans and chimpanzees. *Mol. Biol. Evol.*, **10**, 512–526.
45. Grundy,F.J., Winkler,W.C. and Henkin,T.M. (2002) tRNA-mediated transcription antitermination *in vitro*: codon–anticodon pairing independent of the ribosome. *Proc. Natl Acad. Sci. U.S.A.*, **99**, 11121–11126.

46. Samuels,M., Fire,A. and Sharp,P.A. (1984) Dinucleotide priming of transcription mediated by RNA polymerase II. *J. Biol. Chem.*, **259**, 2517–2525.
47. Saad,N.Y., Stamatopoulou,V., Braye,M., Drainas,D., Stathopoulos,C. and Becker,H.D. (2013) Two-codon T-box riboswitch binding two tRNAs. *Proc. Natl Acad. Sci. U.S.A.*, **110**, 12756–12761.
48. Green,N.J., Grundy,F.J. and Henkin,T.M. (2010) The T box mechanism: tRNA as a regulatory molecule. *FEBS Lett.*, **584**, 318–324.
49. Wencker,F.D.R., Marincola,G., Schoenfelder,S.M.K., Maaß,S., Becher,D. and Ziebuhr,W. (2021) Another layer of complexity in *Staphylococcus aureus* methionine biosynthesis control: unusual RNase III-driven T-box riboswitch cleavage determines met operon mRNA stability and decay. *Nucleic Acids Res.*, **49**, 2192–2212.
50. Schneider,T., Senn,M.M., Berger-Bächi,B., Tossi,A., Sahl,H.G. and Wiedemann,I. (2004) *In vitro* assembly of a complete, pentaglycine interpeptide bridge containing cell wall precursor (lipid II-Gly5) of *Staphylococcus aureus*. *Mol. Microbiol.*, **53**, 675–685.
51. Dare,K. and Ibba,M. (2012) Roles of tRNA in cell wall biosynthesis. *Wiley Interdiscip. Rev. RNA*, **3**, 247–264.
52. Grigg,J.C. and Ke,A. (2013) Sequence, structure, and stacking: specifics of tRNA anchoring to the T box riboswitch. *RNA Biol.*, **10**, 1761–1764.
53. Reiter,N.J., Osterman,A., Torres-Larios,A., Swinger,K.K., Pan,T. and Mondragón,A. (2010) Structure of a bacterial ribonuclease P holoenzyme in complex with tRNA. *Nature*, **468**, 784–789.
54. Fei,J., Kosuri,P., MacDougall,D.D. and Gonzalez,R.L. (2008) Coupling of ribosomal L1 stalk and tRNA dynamics during translation elongation. *Mol. Cell*, **30**, 348–359.
55. Zhang,J. (2021) Interplay between host tRNAs and HIV-1: a structural perspective. *Viruses*, **13**, 1819.
56. Hammond,J.A., Rambo,R.P., Filbin,M.E., Hammond,J.A., Rambo,R.P., Filbin,M.E. and Kieft,J.S. (2009) Comparison and functional implications of the 3D architectures of viral tRNA-like structures comparison and functional implications of the 3D architectures of viral tRNA-like structures. *RNA*, **15**, 294–307.
57. Zhang,J. and Landick,R. (2016) A two-way street: regulatory interplay between RNA polymerase and nascent RNA structure. *Trends Biochem. Sci.*, **41**, 293–310.
58. Grundy,F.J. and Henkin,T.M. (2004) Kinetic analysis of tRNA-directed transcription antitermination of the *Bacillus subtilis* glyQS gene *in vitro*. *J. Bacteriol.*, **186**, 5392–5399.
59. Deigan,K.E. and Ferré-D'Amaré,A.R. (2011) Riboswitches: discovery of drugs that target bacterial gene-regulatory RNAs. *Acc. Chem. Res.*, **44**, 1329–1338.
60. Dar,D., Shamir,M., Mellin,J.R., Koutero,M., Stern-Ginossar,N., Cossart,P. and Sorek,R. (2016) Term-seq reveals abundant ribo-regulation of antibiotics resistance in bacteria. *Science*, **352**, aad9822.
61. Rekand,I.H. and Brenk,R. (2017) Ligand design for riboswitches, an emerging target class for novel antibiotics. *Future Med. Chem.*, **9**, 1649–1662.
62. Frohlich,K.M., Weintraub,S.F., Bell,J.T., Todd,G.C., Väre,V.Y.P., Schneider,R., Kloos,Z.A., Tabe,E.S., Cantara,W.A., Stark,C.J. *et al.* (2019) Discovery of small-molecule antibiotics against a unique tRNA-mediated regulation of transcription in Gram-positive bacteria. *ChemMedChem*, **14**, 758–769.
63. Väre,V.Y.P., Schneider,R.F., Kim,H., Lasek-Nesselquist,E., McDonough,K.A. and Agris,P.F. (2020) Small-molecule antibiotics inhibiting tRNA-regulated gene expression is a viable strategy for targeting Gram-positive bacteria. *Antimicrob. Agents Chemother.*, **65**, e01247-20.